

# Biaxial Constrained Recovery in Shape Memory Alloy Rings

TOMAZ VIDENIC, FRANC KOSEL,\* VIKTOR SAJN AND MIHA BROJAN

*Faculty of Mechanical Engineering, University of Ljubljana, Askerceva 6  
1000 Ljubljana, Slovenia*

**ABSTRACT:** In this article biaxial constrained recovery in a thick-walled shape memory alloy (SMA) ring with a rectangular cross-section is modeled using the theory of generalized plasticity, which is developed by Jacob Lubliner and Ferdinando Auricchio. As a mechanical obstacle that delays free recovery in a SMA ring, a steel ring is used. The result of constrained recovery is the generation of high stresses in both the rings. All equations are written in a closed form in terms of infinite series. Theoretical results are compared with experimental findings and good agreement is found when SMA rings are in the domain of recoverable strains.

*Key Words:* shape memory alloy, mathematical modeling, phase transformation, rings, constrained recovery, generalized plasticity.

## INTRODUCTION

SMART materials are receiving great attention nowadays, mainly for their possible innovative use in practical applications. One example of such materials is the family of shape memory alloys (SMA), which have an intrinsic capacity to return to a previously defined shape by increasing the metal's temperature. This effect arises from reversible and usually rate-independent martensitic transformation and resulting changes of crystal structure of the solid phases of the material. A low-temperature phase is called martensite and a high one is austenite. Large residual strains of even 10% can be recovered in this way and the process is often referred as free recovery. The return to the original shape begins at a temperature called austenite start transformation temperature  $A_S$ , and completes at the austenite finish transformation temperature  $A_f$ . If the free recovery is hampered by an external obstacle before temperature  $A_f$  is reached, the process is called constrained recovery and large stresses, up to 800 MPa, can be generated in SMA elements. This property makes SMA ideally suited for use as fasteners, seals, connectors, and clamps (Kapgan and Melton, 1990; Otsuka and Wayman, 1999). On the other hand, if the SMA is cooled from the fully austenitic phase, it starts to transform back to martensite at a temperature called martensite start transformation temperature  $M_S$ , and ends at the martensite finish transformation temperature  $M_f$ .

The structure obtained in this way is often called the multi-variant martensite. Besides the martensitic transformations associated with the thermal regime, they can be triggered by mechanical loading and the martensite obtained in this way is then called the stress-induced or oriented martensite. The process of constrained recovery is possible only if the structure of SMA is stress-induced or oriented martensite. Another important property of SMA is its superelastic effect. At constant high temperature, above temperature  $A_f$ , a mechanical loading–unloading cycle induces highly nonlinear large deformations. At the end of the loading–unloading cycle no permanent deformations are present. The cycle usually presents a hysteresis loop.

Shape memory alloys have been studied experimentally for the last four decades and numerous constitutive models have been proposed over the last 20 years. The existing models follow either a macroscopic phenomenological or a micromechanical approach. Uniaxial phenomenological models are suitable for engineering practice, because they make use of measurable quantities as parameters and are often relatively simple (see, for example, Tanaka, 1986; Liang and Rogers, 1990; Brinson, 1993; Ivshin and Pence, 1994; Auricchio and Lubliner, 1997). Many efforts have been made to extend these models to three dimensions, but it is difficult to evaluate the performance of three-dimensional phenomenological models due to the lack of experimental data for multiaxial response of SMAs. Three-dimensional phenomenological models have been developed in the form of plasticity models with an internal variable such as the mass fraction of martensite  $\xi$  (see, Auricchio, 1995; Boyd and Lagoudas, 1996a,b;

\* Author to whom correspondence should be addressed.  
E-mail: franc.kosel@fs.uni-lj.si  
Figures 3–8 appear in color online: <http://jim.sagepub.com>

Leclercq and LExcellent, 1996; Lubliner and Auricchio, 1996; Panoskaltis et al., 2004; Lagoudas et al., 2006) and most have been compared only to uniaxial experimental data. The researchers following a micro-mechanics approach (Kafka, 1994; Tokuda et al., 1998; Huang et al., 2000; Thamburaja and Anand, 2001; Novak and Šittner, 2004; Zhu and Liew, 2004; Lagoudas et al., 2006; Patoor et al., 2006) tried to follow very closely the crystallographic phenomena within the material, using thermodynamics laws to describe the transformation. In general, these models are more complicated than the phenomenological models and much more computationally demanding. An interesting result of combining the phenomenological and micromechanical approach is a microplane model for SMA (Brocca et al., 2002). While in the usual phenomenological models the constitutive laws are expressed in terms of stress and strain, in a microplane model the macroscopic material behavior is obtained by describing the material response along several planes of different crystallographic orientations, called the microplanes. To the authors' judgment, the phenomenological model of generalized plasticity (Auricchio, 1995; Lubliner and Auricchio, 1996; Auricchio and Lubliner 1997; Panoskaltis et al., 2004) is well suited for the modeling of biaxial constrained recovery in SMA rings since it is in good agreement with the experimental results and allows the solution, under some simplifications adopted, in a closed form. It is based on some fundamental axioms and on the results from elementary set theory and topology.

The principal aim of the present study is to develop a mathematical model of the biaxial or plane constrained recovery in SMA rings, using the generalized plasticity theory. Available publications on the process of constrained recovery are mostly limited only to uniaxial examples (Edwards et al., 1975; Mohamed, 1978; Furuya et al., 1988; Madangopal et al., 1988; Liang and Rogers, 1990; Proft and Duerig, 1990; Brinson, 1993; Stalmans et al., 1995, 1997; Leclercq and LExcellent, 1996; Šittner et al., 2000; Tsoi et al., 2002; Kato et al., 2004; Novak and Šittner, 2004; Kosel and Videnic, 2007) which is unusual because some of the most successful applications of the SMA to date are tube couplings (Borden, 1990; Kapgan and Melton, 1990). Recently, two articles have been published where SMA rings were constrained to recover in axial direction so that a uniaxial model can be used (Ghorashi and Inman, 2004; Hesse et al., 2004). To the authors' knowledge, a mathematical model of plane constrained recovery in SMA rings is still missing. Some efforts were made to develop a model of constrained recovery in SMA rings (Nagaya and Hirata, 1992) but, again, it is uniaxial in nature since radial stresses are neglected and only circular stresses are taken into account. This simplification is valid only in the case of thin-walled SMA rings.

In this study, a ring made of an ordinary steel material is used as a mechanical obstacle which delays free recovery in an SMA ring. The data for the commercial  $\text{Ni}_{48}\text{Ti}_{38}\text{Nb}_{14}$  SMA ring and the steel ring are fed into the mathematical model in order to generate the system's response. Theoretical results are compared with experimental findings, for this purpose six commercial SMA rings were subjected to constrained recovery and one SMA ring was heated without a mechanical obstacle (free recovery) in order to get the data for four parameters  $\alpha$ ,  $\lambda_M$ ,  $m$ , and  $n$  which are needed in the mathematical model.

## GENERALIZED PLASTICITY IN SHAPE MEMORY MATERIALS

Generalized plasticity is an internal-variable model of rate-independent inelasticity that includes classical plasticity as a special case and was developed in order to model the behavior of elastic-plastic solids in which, following initial plastic loading and elastic unloading, the reloading is not necessarily elastic up to the state at which unloading began. Such solids include graphite, some stainless steels, some rocks, and also SMA. Application of generalized plasticity to the multiaxial behavior of SMAs can be found in Auricchio (1995) and Lubliner and Auricchio (1996), and is presented here only briefly.

Four functions bounded by two bands of straight lines in the effective stress  $\sigma_e$ -temperature  $T$  plane are introduced:

$$F_1 = \sigma_e - C(T - M_f) \quad (1)$$

$$F_2 = \sigma_e - C(T - M_s) \quad (2)$$

$$F_3 = \sigma_e - C(T - A_s) \quad (3)$$

$$F_4 = \sigma_e - C(T - A_f) \quad (4)$$

where  $C$  is the stress rate and is almost the same in both phase transformations (austenite  $\rightarrow$  martensite and martensite  $\rightarrow$  austenite). The loading surfaces are given by:

$$F = \sigma_e - CT = \text{const.} \quad (5)$$

The geometry of the regions is shown in Figure 1. In a two-phase system, it can be assumed that the only internal variable is the fraction of mass occupied by one of the phases. In SMA models this variable is usually the mass fraction of martensite  $\xi$ , with  $\xi = 0$  denoting all austenite and  $\xi = 1$  all martensite. A single internal variable model is suitable for modeling constrained recovery since there is no conversion between martensite variants.

In crystalline solids, the elastic part of strain tensor  $\varepsilon_{ij}^{\text{el}}$  is insensitive to irreversible processes and its dependence on the internal variable  $\xi$  can be neglected (Lubliner, 1972):

$$\varepsilon_{ij} = \varepsilon_{ij}^{\text{el}}(\sigma_{ij}; T) + \varepsilon_{ij}^{\text{iel}}(\xi) \quad (6)$$

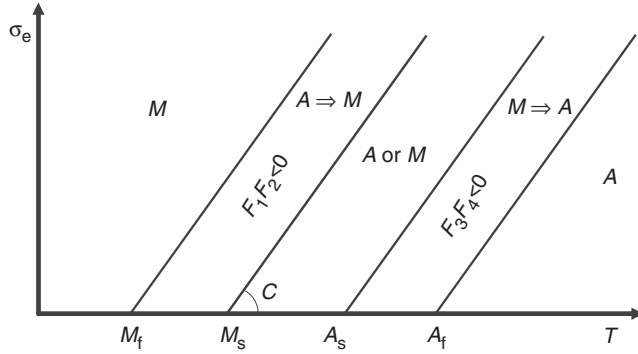


Figure 1. Inelastic domains for austenite to martensite and martensite to austenite transformations.

where  $\varepsilon_{ij}^{iel}$  is the inelastic strain tensor and can be in the case of radial or proportional loading calculated from:

$$\varepsilon_{ij}^{iel} = \lambda \frac{\partial F}{\partial \sigma_{ij}} \quad (7)$$

where  $\lambda$  is a scalar and  $F$  is the inelastic potential defined by Equation (5). Scalar  $\lambda$  is a function of the internal variable  $\xi$ :

$$\lambda = \lambda_M \xi \quad (8)$$

where  $\lambda_M$  is a constant which must be determined experimentally. In the case of uniaxial loading, Equation (8) becomes  $\varepsilon^{iel} = \varepsilon_M \xi$ , where constant  $\varepsilon_M$  is the maximum inelastic strain, attained when the solid is all martensite, and disappears when heated above  $A_f$ . It can be measured by uniaxial tensile experiments. Generally, constant  $\lambda_M$  has to be measured during multiaxial loading and its determination is not as simple as in the uniaxial case.

In the inelastic potential (5) effective stress  $\sigma_e$  should be defined. In the case of constrained recovery in a SMA ring only two components of a stress tensor are not equal to zero: normal radial stress  $\sigma_r$  and normal circular stress  $\sigma_\varphi$ . If  $\sigma_\varphi \geq 0$  and  $\sigma_r \leq 0$ , the effective stress can be defined in the next form:

$$\sigma_e = \sigma_\varphi - \sigma_r + \alpha(\sigma_r + \sigma_\varphi) \quad (9)$$

where  $\alpha$  is the measure of unequal response in tension and compression and should be determined experimentally. The special case  $\alpha=0$  corresponds to equal response; the inelastic potential  $F$  is then of Tresca type. The choice of effective stress in the form (9) allows constrained recovery in an SMA ring to be solved in a closed form. If the inelastic potential would be chosen in a Drucker–Prager form (Lubliner and Auricchio, 1996), the numerical methods should be used and solution in a closed form is not possible.

In the region where phase transformation from martensite to austenite may take place a stress decrease at constant temperature, a temperature increase at constant stress, or a proper combination of these actions

should occur. The conditions for phase transformation can be mathematically written as:

$$F_3 < 0, \quad F_4 > 0 \Rightarrow F_3 F_4 < 0 \text{ and } \dot{F} < 0. \quad (10)$$

The linear flow rule for  $\xi$  can be written in the form (Auricchio, 1995):

$$\dot{\xi} = -\xi \frac{\langle -F_3 F_4 \rangle \langle -\dot{F} \rangle}{|F_3 F_4| F_4} \quad (11)$$

where  $\langle \cdot \rangle$  is the Macaulay bracket, that is  $\langle x \rangle = (x + |x|)/2$ . Flow rule (11) can be integrated in closed form, and assuming initial condition  $\xi = \xi_0$  at  $F_3 = 0$  the solution is:

$$\xi = \xi_0 \frac{\sigma_e - C(T - A_f)}{C(A_f - A_s)}. \quad (12)$$

Since constrained recovery in SMA rings will be dealt with, Equation (12) can be rewritten as:

$$\xi(r; T) = \xi_0(r) \frac{\sigma_e(r; T) - C(T - A_f)}{C(A_f - A_s)} \quad (13)$$

where  $r$  is the radius of the SMA ring.

### MODELING OF CONSTRAINED RECOVERY IN SMA RING

The entire process of constrained recovery can be represented in six steps: (1) An SMA ring is cooled from austenite to multi-variant martensite at zero stress. (2) The SMA ring is widened in a martensitic region (stress-induced or oriented martensite) at a constant temperature. (3) The SMA ring and ordinary steel ring are then heated, and until temperature  $A_s$  is reached both elements extend. (4) At temperature  $A_s$  the SMA ring starts to contract, while the ordinary ring still extends until at temperature  $T_C$  both elements touch each other and the process of constrained recovery in the SMA ring begins. (5) Above temperature  $T_C$ , retransformation to austenite is constrained and continues until temperature  $T_{SE}$  at which the retransformation in the SMA ring is completed. The stresses in the SMA ring increase, therefore temperature  $T_{SE}$  is considerably higher than  $A_f$ . (6) Both rings are cooled down to the end temperature  $T_{end}$ , which can be equal to the ambient temperature  $T_0$ , and are still in contact. Since temperature  $M_s(\sigma_e)$  is lower than  $T_0$ , the transformation from austenite to martensite and consequently relaxation of stresses in the SMA ring does not begin.

The first two steps will not be dealt with in this study, since commercial  $Ni_{48}Ti_{38}Nb_{14}$  SMA rings in the widened ‘ready to use’ martensitic state are available from Intrinsic Devices Inc. The geometry of both rings in different temperature regions is shown in Figure 2.

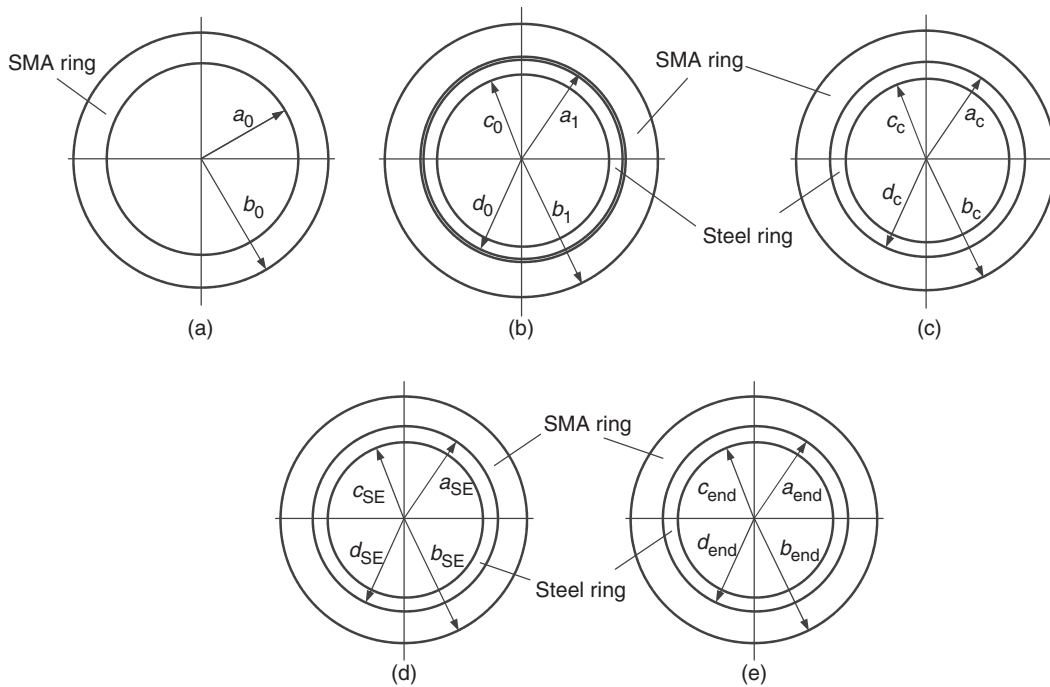


**Figure 2.** Geometry of both rings at different temperatures: (a) before stretching of the SMA ring in martensitic state at constant temperature inner and outer radii are  $a_0$  and  $b_0$ ; (b) geometry of both rings at ambient temperature  $T_0$  after stretching and unloading of the SMA ring. The SMA ring is in martensitic and widened state  $a_1 > d_0 > a_0$ ; (c) at temperature  $T_c$  the rings touch each other; (d) the SMA ring transformation to austenite is finished at temperature  $T_{SE}$ . Large stresses occur in both rings; (e) rings are cooled down to the end temperature  $T_{end}$ , which can be equal to the ambient temperature  $T_0$ .

The state before the stretching–unloading cycle in the martensite condition at ambient temperature  $T_0$  is taken as the reference state in the SMA ring (Figure 2a). In this state all strains are zero. After the stretching–unloading cycle in the martensite condition, the inner and outer radii of the SMA ring at ambient temperature  $T_0$  are  $a_1$  and  $b_1$  (Figure 2b). The reference state in the steel ring is at ambient temperature  $T_0$ , when the inner and outer radii are  $c_0$  and  $d_0$  (Figure 2b). The inelastic normal circular strains  $\varepsilon_{\varphi 0}^{iel}$  at inner and outer radii  $a_0$  and  $b_0$  before retransformation to austenite are:

$$\varepsilon_{\varphi 0}^{iel}(a_0) = \frac{a_1 - a_0}{a_0}. \quad (14)$$

$$\varepsilon_{\varphi 0}^{iel}(b_0) = \frac{b_1 - b_0}{b_0}. \quad (15)$$

The inelastic strains defined in Equations (14) and (15) can be recovered, if heated above temperature  $A_f$ , i.e., during free recovery. These two values must be known, if one wants to model constrained recovery in SMA rings. Commercial  $\text{Ni}_{48}\text{Ti}_{38}\text{Nb}_{14}$  SMA rings in widened state (radii  $a_1$  and  $b_1$ ) are available in the market. Since radii  $a_0$  and  $b_0$  are not known, they can be obtained, if the SMA ring is heated above temperature  $A_f$  and then cooled down to ambient temperature  $T_0$ .

In the first temperature region  $T_0 \leq T \leq A_S$  two material constants  $\lambda_M$  and  $\alpha$ , which are needed in the

mathematical model, are determined from Equations (8) and (9).

### Temperature Region $T_0 \leq T \leq A_S$

Both rings extend during heating and the recovery in the SMA ring from martensite to austenite has not started yet. It is assumed that the stress state in both rings is zero. This is not entirely true since in the SMA ring after loading–unloading cycle some residual stresses must be present. As there is not enough data about the loading–unloading cycle and for reasons of simplicity, these stresses are neglected. The total radial and circular strains  $\varepsilon_r$  and  $\varepsilon_\varphi$  in an SMA ring can be obtained from Equations (6)–(9):

$$\varepsilon_r(r; T) = \varepsilon_{r0}^{iel}(r) + \alpha_S(T - T_0) = \frac{\partial u}{\partial r} \quad (16)$$

$$\varepsilon_r(r; T) = \lambda_M \xi_0(r)(\alpha - 1) + \alpha_S(T - T_0)$$

$$\varepsilon_\varphi(r; T) = \varepsilon_{\varphi 0}^{iel}(r) + \alpha_S(T - T_0) = \frac{u}{r} \quad (17)$$

$$\varepsilon_\varphi(r; T) = \lambda_M \xi_0(r)(1 + \alpha) + \alpha_S(T - T_0)$$

where  $\xi_0(r)$  is the initial mass fraction of stress-induced or oriented martensite variants after the widening process of the SMA ring,  $\alpha_S$  is the linear thermal expansion coefficient of the SMA ring, and  $u$  is the radial displacement in the SMA ring. Note that inelastic strains in Equations (16) and (17) do not vary with

temperature  $T$  in this region, since transformation to austenite has not started yet. From Expressions (16) and (17) one can deduce the following differential equation:

$$(1 + \alpha)r \frac{d\xi_0}{dr} + 2\xi_0 = 0 \quad (18)$$

$$\xi_0(r) = Kr^{-2/(1+\alpha)} \quad (19)$$

where  $K$  is an unknown constant. According to Equation (19), distribution of oriented martensite variants in the SMA ring can be determined. It is assumed that only at inner radius  $a_0$ , the SMA ring contains 100% oriented martensite variants,  $\xi_0(a_0) = 1$ . At all other radii the ring contains a mixture of austenite or multi-variant martensite and oriented martensite,  $\xi_0(r) < 1$ ;  $r \neq a_0$ . This assumption is correct in the case of a thick-walled SMA ring when during the process of a widening excessive loads would be needed for a structure to be 100% oriented martensite throughout the SMA ring (Videnic, 2004). The above considerations can be written mathematically as:

$$\begin{aligned} \varepsilon_{\varphi 0}^{iel}(a_0) &= \lambda_M(1 + \alpha) K b_0^{-2/(1+\alpha)} = \xi_0(b_0) \\ \varepsilon_{\varphi 0}^{iel}(b_0) &= \lambda_M(1 + \alpha) \xi_0(b_0) K a_0^{-2/(1+\alpha)} = 1. \end{aligned}$$

Four unknowns  $\lambda_M$ ,  $\alpha$ ,  $K$ , and  $\xi_0(b_0)$  can be easily determined from the above boundary conditions:

$$\alpha = \frac{2 \log(a_0/b_0)}{\log\left[\frac{\varepsilon_{\varphi 0}^{iel}(b_0)}{\varepsilon_{\varphi 0}^{iel}(a_0)}\right]} - 1. \quad (20)$$

$$\lambda_M = \frac{\varepsilon_{\varphi 0}^{iel}(a_0)}{1 + \alpha}. \quad (21)$$

$$K = a_0^{2/(1+\alpha)}. \quad (22)$$

$$\xi_0(b_0) = \frac{\varepsilon_{\varphi 0}^{iel}(b_0)}{\varepsilon_{\varphi 0}^{iel}(a_0)}. \quad (23)$$

In this way the deformation and displacement state in the SMA ring can be calculated from Equations (16) and (17) since material constants  $\lambda_M$  and  $\alpha$  are known from Equations (20) and (21). Deformation state in a steel ring can be determined from simple expressions:

$$\varepsilon_r^{st}(r; T) = \alpha_{st}(T - T_0) \quad (24)$$

$$\varepsilon_{\varphi}^{st}(r; T) = \alpha_{st}(T - T_0) \quad (25)$$

where  $\alpha_{st}$  is the linear thermal expansion coefficient of the steel ring.

### Temperature Region $A_S \leq T \leq T_C$

At temperature  $A_S$  the SMA ring starts to contract, i.e., the process of the free recovery begins, while the steel ring is extending. At temperature  $T_C$  the rings meet each other. Depending upon the gap between SMA and steel ring, contact temperature  $T_C$  falls anywhere between temperatures  $A_S$  and  $A_f$ . As in the previous

temperature region, the stress state is zero in both rings. Using Equations (6)–(8), (13), (19), and (22), the deformation state in the SMA ring is:

$$\varepsilon_r(r; T) = \lambda_M(\alpha - 1) \left(\frac{a_0}{r}\right)^{2/(1+\alpha)} \frac{A_f - T}{A_f - A_S} + \alpha_S(T - T_0). \quad (26)$$

$$\varepsilon_{\varphi}(r; T) = \lambda_M(1 + \alpha) \left(\frac{a_0}{r}\right)^{2/(1+\alpha)} \frac{A_f - T}{A_f - A_S} + \alpha_S(T - T_0). \quad (27)$$

As in the previous temperature region the deformation state in the steel ring can be calculated from Equations (24) and (25). The contact temperature  $T_C$  can be calculated from the condition of equal radii  $a_C$  and  $d_C$  (Figure 2c) using Equations (25) and (27):

$$T_C = \frac{[(1 - \alpha_{st}T_0)d_0 - (1 + \alpha_S T_0)a_0](A_f - A_S) - \lambda_M(1 + \alpha)A_f a_0}{(\alpha_S a_0 - \alpha_{st}d_0)(A_f - A_S) - \lambda_M(1 + \alpha)a_0}. \quad (28)$$

### Temperature Region $T_C \leq T \leq T_{SE}$

From the temperature  $T_C$  onwards the SMA ring and the steel ring are in contact, since the SMA ring wants to shrink to the geometry before loading–unloading process (Figure 2a). At the same time the steel ring wants to expand and great stresses are generated in both rings. The boundary condition of equal inner radius of the SMA ring and outer radius of the steel ring,  $a(T) = d(T)$ , can be written as:

$$\begin{aligned} a(T) &= d_C + \alpha_{st}(T - T_C)d_C \\ &+ \frac{d_C}{E_{st}} [(1 - \nu_{st})A_{st} - (1 + \nu_{st})B_{st}d_C^{-2}] \end{aligned} \quad (29)$$

where  $E_{st}$  is the Young's modulus of the steel ring,  $\nu_{st}$  is the Poisson's ratio of the steel ring, and  $A_{st}$ ,  $B_{st}$  are unknowns which vary with temperature  $T$ . In Equation (29) elastic strains are assumed in the steel ring during the whole process of constrained recovery in the SMA ring. Radial and circular stresses in the steel ring can be therefore written as:

$$\sigma_r^{st}(r; T) = A_{st}(T) + B_{st}(T)r^{-2}. \quad (30)$$

$$\sigma_{\varphi}^{st}(r; T) = A_{st}(T) - B_{st}(T)r^{-2}. \quad (31)$$

Unknowns  $A_{st}$  and  $B_{st}$  can be determined from boundary conditions  $\sigma_r^{st}(c_C; T) = 0$  and  $\sigma_r^{st}(d_C; T) = -p_0(T)$  as:

$$A_{st}(T) = -\frac{d_C^2}{d_C^2 - c_C^2} p_0(T). \quad (32)$$

$$B_{st}(T) = \frac{c_C^2 d_C^2}{d_C^2 - c_C^2} p_0(T). \quad (33)$$

It should be noted that contact pressure  $p_0(T)$  between both rings is not known yet. Unknowns (32) and (33) are inserted into Equation (29) and then the expression for circular strain in the SMA ring  $\varepsilon_\varphi(a_0; T) = [a(T) - a_0]/a_0$  can be written as:

$$\varepsilon_\varphi(a_0; T) = C_1 + C_2 T + C_3 \sigma_r(a_0; T) \quad (34)$$

where the expression  $\sigma_r(a_0; T) = -p_0(T)$  is considered and constants  $C_1$ ,  $C_2$ , and  $C_3$  are:

$$C_1 = (1 - \alpha_{st} T_C) \frac{dC}{a_0} - 1, \quad C_2 = \alpha_{st} \frac{dC}{a_0}, \quad (35)$$

$$C_3 = \frac{(1 - \nu_{st}) d_C^2 + (1 + \nu_{st}) c_C^2 dC}{(d_C^2 - c_C^2) E_{st} a_0}. \quad (36)$$

Circular strain (34) can also be written, according to Equation(6), as:

$$\begin{aligned} \varepsilon_\varphi(a_0; T) &= \varepsilon_\varphi^{iel}(a_0; T) + \varepsilon_\varphi^{el}(a_0; T) \\ \frac{\partial \varepsilon_\varphi}{\partial T} \Big|_{a_0; T} &= \lambda_M (1 + \alpha) \frac{\partial \xi}{\partial T} \Big|_{a_0; T} \\ &+ \alpha_S + \frac{1}{E_S} \left( \frac{\partial \sigma_\varphi^{el}}{\partial T} \Big|_{a_0; T} - \nu_S \frac{\partial \sigma_r^{el}}{\partial T} \Big|_{a_0; T} \right) \end{aligned} \quad (37)$$

with  $E_S$  and  $\nu_S$  the Young's modulus and the Poisson's ratio of the SMA ring, respectively. It must be noted that elastic stresses  $\sigma_r^{el}$  and  $\sigma_\varphi^{el}$  are not true stresses ( $\sigma_r$  and  $\sigma_\varphi$  are true stresses) in the SMA ring. The distinction between  $\sigma^{el}$  and  $\sigma$  originates from theoretical treatment of uniaxial constrained recovery proposed by Rudy Stalmans and his colleagues (Stalmans et al., 1995, 1997). An infinitesimal temperature increase  $dT$  induces a stress increase  $d\sigma$  and a change of mass fraction of martensite  $\xi$ . They achieved this infinitesimal step from  $(T, \sigma, \xi)$  to  $(T + dT, \sigma + d\sigma, \xi + d\xi)$  in two intermediate steps. The first step is a temperature increase  $dT$  at constant  $\xi$  which yields an increase of the stress by  $d\sigma^{el}$ . The second step is unloading at constant temperature  $T + dT$ . Similarly, in the case of a biaxial constrained recovery in SMA rings it can be written using Equation (9):

$$C = \frac{\partial \sigma_\varphi^{el}}{\partial T} = \frac{\partial \sigma_\varphi^{el}}{\partial T} - \frac{\partial \sigma_r^{el}}{\partial T} + \alpha \left( \frac{\partial \sigma_r^{el}}{\partial T} + \frac{\partial \sigma_\varphi^{el}}{\partial T} \right) \quad (38)$$

$$C = m \frac{\partial \sigma_\varphi^{el}}{\partial T} = -n \frac{\partial \sigma_r^{el}}{\partial T} \quad (39)$$

with  $m$  and  $n$  as unknowns which can be determined using Equations (38) and (39) and from Equations  $\sigma_r^{el} = A + Br^{-2}$ ,  $\sigma_\varphi^{el} = A - Br^{-2}$ , and boundary conditions  $\sigma_r^{el}(a_0; T) = -p(T)$  and  $\sigma_r^{el}(b_0; T) = 0$ :

$$m(r) = 2 \frac{b_0^2 + \alpha r^2}{b_0^2 + r^2}; \quad a_0 \leq r \leq b_0. \quad (40)$$

$$n(r) = 2 \frac{b_0^2 + \alpha r^2}{b_0^2 - r^2}; \quad a_0 \leq r \leq b_0. \quad (41)$$

Expression (34) is differentiated with respect to temperature  $T$  and then equated with Equation (37) where Equations (40) and (41) are used:

$$\begin{aligned} \frac{\partial \xi}{\partial T} \Big|_{a_0; T} &= \frac{1}{\lambda_M (1 + \alpha)} \\ &\times \left[ C_3 \frac{\partial \sigma_r}{\partial T} \Big|_{a_0; T} + C_2 - \alpha_S - \frac{C [n(a_0) + \nu_S m(a_0)]}{E_S m(a_0) n(a_0)} \right]. \end{aligned} \quad (42)$$

Using Equations (9), (13), and equilibrium equation  $\sigma_\varphi = r \partial \sigma_r / \partial r + \sigma_r$  it can be written that:

$$\frac{\partial \xi}{\partial T} \Big|_{a_0; T} = \left[ (1 + \alpha) a_0 \frac{\partial^2 \sigma_r}{\partial r \partial T} \Big|_{a_0; T} + 2\alpha \frac{\partial \sigma_r}{\partial T} \Big|_{a_0; T} - C \right] \frac{1}{C(A_f - A_S)}. \quad (43)$$

Equations (42) and (43) can be equated and then integrated with respect to temperature from  $T_C$  to  $T$ . Using boundary conditions  $\partial \sigma_r / \partial r \Big|_{a_0; T_C} = 0$  and  $\sigma_r(a_0; T_C) = 0$ , it can be written that:

$$\begin{cases} (1 + \alpha) a_0 \frac{\partial \sigma_r}{\partial r} \Big|_{a_0; T} + \left( 2\alpha - \frac{CC_3(A_f - A_S)}{\lambda_M(1 + \alpha)} \right) \sigma_r(a_0; T) \\ = C \left[ \frac{A_f - A_S}{\lambda_M(1 + \alpha)} \left( C_2 - \alpha_S - \frac{C}{E_S} \frac{n(a_0) + \nu_S m(a_0)}{m(a_0)n(a_0)} \right) + 1 \right] \\ \times (T - T_C). \end{cases} \quad (44)$$

There are two unknowns in Equation (44):  $\partial \sigma_r / \partial r \Big|_{a_0; T}$  and  $\sigma_r(a_0; T)$ , so other equations are needed to solve the problem of plane constrained recovery in SMA rings. Similar equation can be derived in the case of uniaxial constrained recovery (Kosel and Videnic, 2007) where such equation fully depicts the process and no additional expressions are needed. It will be shown that the Expression (44) represents one of the three boundary conditions since it is valid only at the inner radius  $a_0$  of the SMA ring. At an arbitrary radius  $r$ , it is possible to write a similar equation as Equation (37):

$$\begin{aligned} \varepsilon_\varphi = \frac{u}{r} &= \lambda_M (1 + \alpha) \xi + \alpha_S (T - T_0) + \frac{1}{E_S} \left( \sigma_\varphi^{el} - \nu_S \sigma_r^{el} \right) \\ \left\{ \begin{aligned} \frac{\partial^2 u}{\partial r \partial T} &= \lambda_M (1 + \alpha) \frac{\partial \xi}{\partial T} + \frac{1}{E_S} \left( \frac{\partial \sigma_\varphi^{el}}{\partial T} - \nu_S \frac{\partial \sigma_r^{el}}{\partial T} \right) + \alpha_S \\ &+ r \left[ \lambda_M (1 + \alpha) \frac{\partial^2 \xi}{\partial r \partial T} + \frac{1}{E_S} \left( \frac{\partial^2 \sigma_\varphi^{el}}{\partial r \partial T} - \nu_S \frac{\partial^2 \sigma_r^{el}}{\partial r \partial T} \right) \right]. \end{aligned} \right. \end{aligned} \quad (45)$$

Radial strain  $\varepsilon_r(r; T)$  in the SMA ring can be written as:

$$\varepsilon_r = \frac{\partial u}{\partial r} = \lambda_M(\alpha - 1)\xi + \alpha_S(T - T_0) + \frac{1}{E_S}(\sigma_r^{el} - \nu_S\sigma_\varphi^{el})$$

$$\frac{\partial^2 u}{\partial r \partial T} = \lambda_M(\alpha - 1)\frac{\partial \xi}{\partial T} + \alpha_S + \frac{1}{E_S}\left(\frac{\partial \sigma_r^{el}}{\partial T} - \nu_S\frac{\partial \sigma_\varphi^{el}}{\partial T}\right). \tag{46}$$

Expressions (45) and (46) can be equated and after using (39)–(41), it is possible to write:

$$(1 + \alpha)r\frac{\partial^2 \xi}{\partial r \partial T} + 2\frac{\partial \xi}{\partial T} = -\frac{Cb_0^2}{\lambda_M E_S}$$

$$\times \left( \frac{1 + \nu_S}{b_0^2 + \alpha r^2} + \frac{(1 - \alpha - \nu_S(1 + \alpha))r^2}{(b_0^2 + \alpha r^2)^2} \right). \tag{47}$$

Using Expressions (9), (13), and equilibrium equation in differential equation (47) and after integration with respect to temperature from  $T_C$  to  $T$  it can be written that:

$$\left\{ \begin{aligned} &(1 + \alpha)r\frac{\partial^2 \sigma_r}{\partial r^2} + (1 + 3\alpha)\frac{\partial \sigma_r}{\partial r} \\ &= -\frac{C^2(A_f - A_S)a_0^{\frac{-2}{1+\alpha}}b_0^2}{\lambda_M(1 + \alpha)E_S} \\ &\times \left[ \frac{(1 + \nu_S)r^{\frac{1-\alpha}{1+\alpha}}}{b_0^2 + \alpha r^2} + \frac{(1 - \alpha - \nu_S(1 + \alpha))r^{\frac{3+\alpha}{1+\alpha}}}{(b_0^2 + \alpha r^2)^2} \right] (T - T_C). \end{aligned} \right. \tag{48}$$

In differential equation (48) conditions  $\partial^2 \sigma_r / \partial r^2|_{r; T_C} = 0$  and  $\partial \sigma_r / \partial r|_{r; T_C} = 0$  are considered since zero stress state in the SMA ring at contact temperature  $T_C$  is assumed. The solution of the above differential equation is:

$$\left\{ \begin{aligned} &\sigma_r(r; T) \\ &= -\frac{C^2(A_f - A_S)a_0^{\frac{-2}{1+\alpha}}b_0^2}{2\lambda_M\alpha(1 + \alpha)E_S} \\ &\times [(1 + \nu_S)I_2(r) + (1 - \alpha - \nu_S(1 + \alpha))I_4(r)](T - T_C) \\ &+ E_1(T) + E_2(T)r^{\frac{-2\alpha}{1+\alpha}} + \frac{C^2(A_f - A_S)a_0^{\frac{-2}{1+\alpha}}b_0^2}{4\lambda_M\alpha^2(1 + \alpha)E_S} \\ &\times \left[ \frac{1 - \nu_S}{\alpha} \ln \frac{b_0^2 + \alpha r^2}{b_0^2 + \alpha a_0^2} + \frac{(1 - \alpha - \nu_S(1 + \alpha))b_0^2(a_0^2 - r^2)}{(b_0^2 + \alpha r^2)(b_0^2 + \alpha a_0^2)} \right] \\ &\times (T - T_C)r^{\frac{-2\alpha}{1+\alpha}} \end{aligned} \right. \tag{49}$$

with  $I_2(r)$  and  $I_4(r)$  are known functions presented in the Appendix and  $E_1(T)$  and  $E_2(T)$  are unknown functions that can be determined from boundary conditions.

Using the equilibrium equation, circular stress  $\sigma_\varphi$  in the SMA ring can easily be calculated as:

$$\left\{ \begin{aligned} &\sigma_\varphi(r; T) \\ &= -\frac{C^2(A_f - A_S)a_0^{\frac{-2}{1+\alpha}}b_0^2}{2\lambda_M\alpha(1 + \alpha)E_S} [(1 + \nu_S)I_2(r) \\ &+ (1 - \alpha - \nu_S(1 + \alpha))I_4(r)](T - T_C) \\ &+ E_1(T) + \frac{1 - \alpha}{1 + \alpha}E_2(T)r^{\frac{-2\alpha}{1+\alpha}} + \frac{C^2(A_f - A_S)(1 - \alpha)a_0^{\frac{-2}{1+\alpha}}b_0^2}{4\lambda_M\alpha^2(1 + \alpha)^2E_S} \\ &\times \left[ \frac{1 - \nu_S}{\alpha} \ln \frac{b_0^2 + \alpha r^2}{b_0^2 + \alpha a_0^2} + \frac{(1 - \alpha - \nu_S(1 + \alpha))b_0^2(a_0^2 - r^2)}{(b_0^2 + \alpha r^2)(b_0^2 + \alpha a_0^2)} \right] \\ &\times (T - T_C)r^{\frac{-2\alpha}{1+\alpha}}. \end{aligned} \right. \tag{50}$$

Along with the boundary condition (44) it is possible to write down two additional boundary conditions:

$$\left\{ \begin{aligned} &\sigma_r(a_0; T) = -p_0(T) \\ &E_1(T) + E_2(T)a_0^{-2\alpha/(1+\alpha)} + p_0(T) = 0 \end{aligned} \right. \tag{51}$$

$$\sigma_r(b_0; T) = 0 \left\{ \begin{aligned} &E_1(T) + E_2(T)b_0^{\frac{-2\alpha}{1+\alpha}} = \frac{C^2(A_f - A_S)a_0^{\frac{-2}{1+\alpha}}b_0^2}{2\lambda_M\alpha(1 + \alpha)E_S} \\ &\times [(1 + \nu_S)I_2(b_0) + (1 - \alpha - \nu_S(1 + \alpha))I_4(b_0)] \\ &\times (T - T_C) - \frac{C^2(A_f - A_S)}{4\lambda_M\alpha^2(1 + \alpha)E_S} \\ &\times \left[ \frac{1 - \nu_S}{\alpha} \ln \frac{(1 + \alpha)b_0^2}{b_0^2 + \alpha a_0^2} \right. \\ &\left. - \frac{(1 - \alpha - \nu_S(1 + \alpha))(b_0^2 - a_0^2)}{(1 + \alpha)b_0^2(b_0^2 + \alpha a_0^2)} \right] \left( \frac{b_0}{a_0} \right)^{\frac{2}{1+\alpha}} \\ &\times (T - T_C). \end{aligned} \right. \tag{52}$$

Using Equation (49) in Equation (44) it is possible to write:

$$\left\{ \begin{aligned} &2\alpha E_2(T)a_0^{-2\alpha/(1+\alpha)} + \left( 2\alpha - \frac{CC_3(A_f - A_S)}{\lambda_M(1 + \alpha)} \right) p_0(T) \\ &= -C \left[ \frac{A_f - A_S}{\lambda_M(1 + \alpha)} \left( C_2 - \alpha_S - \frac{C}{E_S} \frac{n(a_0) + \nu_S m(a_0)}{m(a_0)n(a_0)} \right) + 1 \right] \\ &\times (T - T_C). \end{aligned} \right. \tag{53}$$

Three unknowns  $E_1(T)$ ,  $E_2(T)$ , and  $p_0(T)$  can be easily determined from Equations (51)–(53) but are not written here since the expressions are cumbersome. Effective stress  $\sigma_e(r; T)$  in the SMA ring can be determined from Equation (9) and martensite fraction  $\xi(r; T)$  from Equation (13) using Equations (19) and (22):

$$\xi(r; T) = \left(\frac{a_0}{r}\right)^{2/(1+\alpha)} \frac{\sigma_e(r; T) - C(T - A_f)}{C(A_f - A_s)}$$

The temperature  $T_{SE}$  at which retransformation from martensite to austenite during constrained recovery is completed can be calculated from the condition  $\xi(r; T_{SE}) = 0$ . Since martensite fraction  $\xi$  is varying with radius  $r$ , the temperature  $T_{SE}$  cannot be easily determined. It can be shown that the retransformation always ends first at outer radius  $r = b_0$  while the structure at other radii is still mixed (martensite and austenite). According to this assumption it is possible to write:

$$\xi(b_0; T_{SE}) = \left(\frac{a_0}{b_0}\right)^{2/(1+\alpha)} \frac{\sigma_e(b_0; T_{SE}) - C(T_{SE} - A_f)}{C(A_f - A_s)} = 0 \tag{54}$$

Owing to simplicity, the temperature  $T_{SE}$  can be calculated from Equation (54), but the expression is not presented here since it is cumbersome. It should be noted that real temperature  $T_{SE}$  is somewhat larger than the one from Equation (54), since at all other radii the structure is still a mixture of martensite and austenite.

In this way the stress–strain state in the SMA ring during constrained recovery is determined. The stress–strain state in the inner steel ring can also be determined from Equations (29)–(33).

**Temperature Region  $T_{SE} \geq T \geq T_{end}$**

The temperature  $T_{SE}$  for a commercial  $Ni_{48}Ti_{38}Nb_{14}$  SMA ring is usually higher than  $100^\circ C$ . It means that the system SMA ring – steel ring must be cooled down to be used at temperature  $T_{end}$ . In this temperature region, both rings contract with decreasing temperature  $T$  since transformation from austenite to martensite in the SMA ring has not started yet. Radial and circular strains in the SMA ring can be written as:

$$\varepsilon_r = \frac{\partial u}{\partial r} = \frac{1}{E_S} (\sigma_r - \nu_S \sigma_\varphi) + \alpha_S (T - T_{SE}) \tag{55}$$

$$\varepsilon_\varphi = \frac{u}{r} = \frac{1}{E_S} (\sigma_\varphi - \nu_S \sigma_r) + \alpha_S (T - T_{SE}) \tag{56}$$

where stresses  $\sigma_r$  and  $\sigma_\varphi$  are real stresses since there is no phase transformation. Similarly as in the previous temperature region, from Equations (55) and (56) and using equilibrium equation it is possible to write:

$$r^2 \frac{\partial^3 \sigma_r}{\partial r^2 \partial T} + 3r \frac{\partial^2 \sigma_r}{\partial r \partial T} = 0. \tag{57}$$

Equation (57) can be integrated with respect to temperature  $T$  from  $T_{SE}$  to  $T$  and after using Equation (49) it is possible to write:

$$\left\{ \begin{aligned} r^2 \frac{\partial^2 \sigma_r}{\partial r^2} + 3r \frac{\partial \sigma_r}{\partial r} &= -\frac{4\alpha}{(1+\alpha)^2} E_2(T_{SE}) r^{\frac{-2\alpha}{1+\alpha}} \\ &- \frac{C^2(A_f - A_s) a_0^{\frac{-2}{1+\alpha}} b_0^2}{\lambda_M \alpha (1+\alpha)^3 E_S} \\ &\times \left[ \frac{1 - \nu_S}{\alpha} \ln \frac{b_0^2 + \alpha r^2}{b_0^2 + \alpha a_0^2} + \frac{(1 - \alpha - \nu_S(1 + \alpha)) b_0^2 (a_0^2 - r^2)}{(b_0^2 + \alpha r^2)(b_0^2 + \alpha a_0^2)} \right] \\ &\times (T_{SE} - T_C) r^{\frac{-2\alpha}{1+\alpha}} - \frac{C^2(A_f - A_s) a_0^{\frac{-2}{1+\alpha}} b_0^2}{\lambda_M \alpha (1+\alpha)^2 E_S} \\ &\times \left[ \frac{(1 - \nu_S) r^{\frac{2}{1+\alpha}}}{b_0^2 + \alpha r^2} - \frac{(1 - \alpha - \nu_S(1 + \alpha)) b_0^2 r^{\frac{2}{1+\alpha}}}{(b_0^2 + \alpha r^2)^2} \right] (T_{SE} - T_C). \end{aligned} \right. \tag{58}$$

The solution of differential equation (58) is:

$$\left\{ \begin{aligned} \sigma_r(r; T) &= E_4(T) + E_3(T) r^{-2} \\ &- \frac{C^2(A_f - A_s) a_0^{\frac{-2}{1+\alpha}} b_0^2}{2\lambda_M \alpha (1+\alpha)^3 E_S} (T_{SE} - T_C) \\ &\times \left[ -\frac{1 - \nu_S}{\alpha r^2} I_1(r) - \frac{1 - \alpha - \nu_S(1 + \alpha)}{b_0^2 + \alpha a_0^2} \left(\frac{b_0}{r}\right)^2 \right. \\ &\times (a_0^2 I_2(r) - I_3(r)) + (1 + \alpha)(1 - \alpha - \nu_S(1 + \alpha)) \left(\frac{b_0}{r}\right)^2 I_4(r) \\ &- \frac{(1 - \nu_S)(1 + \alpha)}{r^2} I_3(r) + (1 - \nu_S)(1 + \alpha) I_2(r) \\ &- b_0^2 (1 + \alpha)(1 - \alpha - \nu_S(1 + \alpha)) I_7(r) \\ &\left. + \frac{1 - \nu_S}{\alpha} I_5(r) + \frac{(1 - \alpha - \nu_S(1 + \alpha)) b_0^2}{b_0^2 + \alpha a_0^2} (a_0^2 I_6(r) - I_2(r)) \right] \\ &+ E_2(T_{SE}) r^{\frac{-2\alpha}{1+\alpha}} \end{aligned} \right. \tag{59}$$

with  $I_1(r)$ ,  $I_3(r)$ ,  $I_5(r)$ ,  $I_6(r)$ , and  $I_7(r)$  are known functions presented in the Appendix and  $E_3(T)$ ,  $E_4(T)$  are unknown functions that can be determined from boundary conditions.

The circular stress in the SMA ring can be derived from equilibrium equation and (59) as:

$$\left\{ \begin{aligned} \sigma_\varphi(r; T) &= E_4(T) - E_3(T)r^{-2} - \frac{C^2(A_f - A_S)a_0^{\frac{-2}{1+\alpha}}b_0^2}{2\lambda_M\alpha(1+\alpha)^3 E_S} \\ &\times (T_{SE} - T_C) \left[ \frac{1 - \nu_S}{\alpha r^2} I_1(r) + \frac{1 - \alpha - \nu_S(1 + \alpha)}{b_0^2 + \alpha a_0^2} \left(\frac{b_0}{r}\right)^2 \right. \\ &\times (a_0^2 I_2(r) - I_3(r)) - (1 + \alpha)(1 - \alpha - \nu_S(1 + \alpha)) \left(\frac{b_0}{r}\right)^2 I_4(r) \\ &+ \frac{(1 - \nu_S)(1 + \alpha)}{r^2} I_3(r) + (1 - \nu_S)(1 + \alpha) I_2(r) \\ &- b_0^2(1 + \alpha)(1 - \alpha - \nu_S(1 + \alpha)) I_7(r) + \frac{1 - \nu_S}{\alpha} I_5(r) \\ &+ \left. \frac{(1 - \alpha - \nu_S(1 + \alpha))b_0^2}{b_0^2 + \alpha a_0^2} (a_0^2 I_6(r) - I_2(r)) \right] \\ &+ \frac{1 - \alpha}{1 + \alpha} E_2(T_{SE})r^{\frac{-2\alpha}{1+\alpha}}. \end{aligned} \right. \quad (60)$$

Two of the three boundary conditions can be easily written as:

$$\sigma_r(a_0; T) = -p_0(T) \quad (61)$$

$$E_4(T) + E_3(T)a_0^{-2} + p_0(T) = E_2(T_{SE})a_0^{-2\alpha/1+\alpha}$$

$$\sigma_r(b_0; T) = 0 \left\{ \begin{aligned} E_4(T) + E_3(T)b_0^{-2} &= \frac{C^2(A_f - A_S)a_0^{\frac{-2}{1+\alpha}}b_0^2}{2\lambda_M\alpha(1+\alpha)^3 E_S} (T_{SE} - T_C) \\ &\times \left[ -\frac{1 - \nu_S}{\alpha b_0^2} I_1(b_0) - \frac{1 - \alpha - \nu_S(1 + \alpha)}{b_0^2 + \alpha a_0^2} \right. \\ &\times (a_0^2 I_2(b_0) - I_3(b_0)) \\ &+ (1 + \alpha)(1 - \alpha - \nu_S(1 + \alpha)) I_4(b_0) \\ &- \frac{(1 - \nu_S)(1 + \alpha)}{b_0^2} I_3(b_0) + (1 - \nu_S)(1 + \alpha) I_2(b_0) \\ &- b_0^2(1 + \alpha)(1 - \alpha - \nu_S(1 + \alpha)) I_7(b_0) \\ &+ \frac{1 - \nu_S}{\alpha} I_5(b_0) + \frac{(1 - \alpha - \nu_S(1 + \alpha))b_0^2}{b_0^2 + \alpha a_0^2} \\ &\times \left. (a_0^2 I_6(b_0) - I_2(b_0)) \right] - E_2(T_{SE})b_0^{\frac{-2\alpha}{1+\alpha}}. \end{aligned} \right. \quad (62)$$

The SMA ring and the steel ring are still in contact and Equation (34) is valid. Equations (34) and (56)

are differentiated with respect to temperature  $T$ , and then equated. After using equilibrium equation, the integration with respect to temperature  $T$  from  $T_{SE}$  to  $T$  can be carried out and then after inserting Equations (49) and (59), the third boundary condition can be written as:

$$\begin{aligned} &2a_0^{-2}E_3(T) + (1 - C_3E_S - \nu_S)p_0(T) \\ &= (1 - C_3E_S - \nu_S)p_0(T_{SE}) - E_S(C_2 - \alpha_S)(T - T_{SE}). \end{aligned} \quad (63)$$

Three unknowns  $E_3(T)$ ,  $E_4(T)$ , and  $p_0(T)$  can be easily determined from boundary conditions (61)–(63) but are not written here since expressions are even more cumbersome than unknowns  $E_1(T)$ ,  $E_2(T)$ , and  $p_0(T)$  in the previous temperature region.

The stress–strain state in the SMA ring is now determined in all four temperature regions. The stress–strain state in the inner steel ring can be determined from Equations (29)–(33) as in the previous temperature region.

### SOME NUMERICAL EXAMPLES AND EXPERIMENTAL RESULTS

The numerical values for SMA material parameters are based on values given by the company, Intrinsic Devices Inc., San Francisco. Some material parameters are approximate, for instance the Young’s modulus of martensite, the Poisson’s ratios, and the linear thermal expansion coefficients. For the sake of simplicity, in the current approach a constant value for Young’s modulus  $E_S$  was chosen for both phases (martensite and austenite). The Young’s modulus for steel was measured on the Zwick Z050 tensile test machine and the other steel material parameters are taken from materials science handbooks. The radii of both the rings were measured on the digital electronic automation (DEA) coordinate measuring machine (error  $\pm 2 \mu\text{m}$ ). The input values are presented in Table 1.

At temperature  $A_S$ , free recovery from martensite to austenite in the SMA ring begins. The inner radius of the SMA ring wants to shrink from  $a_1$  to  $a_0$ . Since the outer radius of the steel ring  $d_0$  is bigger than  $a_0$  both rings contact each other at temperature  $T_C$  and the process of constrained recovery begins. The retransformation ends at temperature  $T_{SE}$ , which is well above  $A_f$ . The system is then cooled down to the end temperature  $T_{end}$ , which will in this case be equal to the ambient temperature  $T_0$ . In order to perform calculations, a computer program was written in Fortran. It should be noted that the program is simple since all equations needed for

**Table 1. Input values for numerical calculation of constrained recovery.**

$a_0 = 9.143$ mm	$b_0 = 16.08$ mm	$a_1 = 9.712$ mm	$b_1 = 16.515$ mm
$c_0 = 7.2135$ mm	$d_0 = 9.2995$ mm	$A_S = 50^\circ\text{C}$	$A_f = 80^\circ\text{C}$
$T_0 = T_{\text{end}} = 20^\circ\text{C}$	$\alpha_{\text{st}} = 1.1 \times 10^{-5} \text{K}^{-1}$	$\alpha_{\text{st}} = 1.15 \times 10^{-5} \text{K}^{-1}$	$C = 5.5 \text{MPa/K}$
$\nu_{\text{st}} = 0.3$	$\nu_{\text{S}} = 0.3$	$E_{\text{st}} = 195 \text{GPa}$	$E_{\text{S}} = 30 \text{GPa}$

**Table 2. Some results of numerical calculation.**

$\varepsilon_{\varphi}^{\text{iel}}(a_0) = 0.06223$	$\varepsilon_{\varphi}^{\text{iel}}(b_0) = 0.02705$	$\alpha = 0.35535$	$\lambda_{\text{M}} = 0.04592$
$m(a_0) = 1.685$	$n(a_0) = 3.295$	$T_{\text{C}} = 71.73^\circ\text{C}$	$T_{\text{SE}} = 119.7^\circ\text{C}$
$E_1(T_{\text{SE}}) = 340.79 \text{MPa}$	$E_2(T_{\text{SE}}) = -1445 \text{Nmm}^{-2/(1+\alpha)}$	$\xi(a_0; T_{\text{SE}}) = 0.1445$	$\xi(b_0; T_{\text{SE}}) = 0$
$p_0(T_{\text{SE}}) = 112.03 \text{MPa}$	$a(T_{\text{SE}}) = d(T_{\text{SE}}) = 9.2903 \text{mm}$	$c(T_{\text{SE}}) = 7.201 \text{mm}$	$E_3(T_{\text{end}}) = 91.63 \text{N}$
$p_0(T_{\text{end}}) = 111.29 \text{MPa}$	$a(T_{\text{end}}) = d(T_{\text{end}}) = 9.280 \text{mm}$	$c(T_{\text{end}}) = 7.193 \text{mm}$	$E_4(T_{\text{end}}) = 340.44 \text{MPa}$

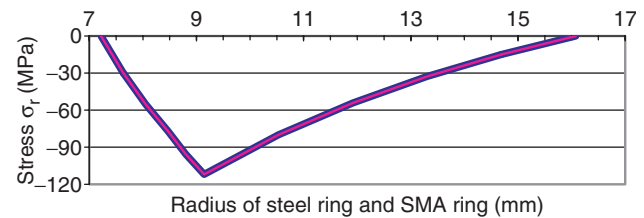
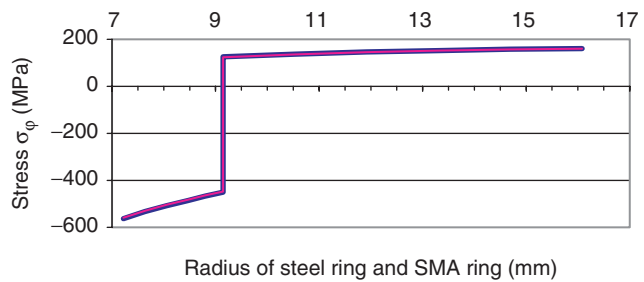
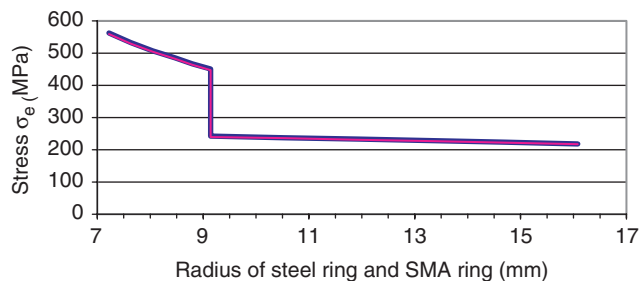
calculation are written in a closed form (but not finite, as can be seen in the Appendix). Some results of numerical calculation are presented in Table 2.

From this table, it can be seen that the stress state at temperature  $T_{\text{SE}}$  is very similar as at the temperature  $T_{\text{end}}$  even though the difference is almost  $100^\circ\text{C}$  (linear thermal expansion coefficients of both materials  $\alpha_{\text{st}}$  and  $\alpha_{\text{S}}$  are similar). Of course, the strain state in the rings is not similar at both temperatures, since rings contract during cooling from  $T_{\text{SE}}$  to  $T_{\text{end}}$ . Figures 3–5 show the distribution of normal radial, circular, and effective stresses in both rings at temperatures  $T_{\text{SE}}$  and  $T_{\text{end}}$ .

From these figures it can be seen that the functions of stresses are equal for both temperatures  $T_{\text{SE}}$  and  $T_{\text{end}}$ , since contact pressure  $p_0(T_{\text{SE}}) \approx p_0(T_{\text{end}})$  and the stress state in both rings are very similar. If linear thermal expansion coefficients of both materials are similar, there is no need to calculate stresses at temperature  $T_{\text{end}}$  from Equations (59) and (60) which are much more complicated than Equations (49) and (50) from which the stress state at temperature  $T_{\text{SE}}$  can be calculated. The effective stress in the steel ring in Figure 5 is calculated from Tresca equation  $\sigma_e^{\text{st}} = -\sigma_{\varphi}^{\text{st}}$ .

Figure 6 shows the relationship between contact pressure  $p_0(T_{\text{end}})$  and outer radius  $d_0$  of the steel ring and between temperature  $T_{\text{SE}}$  and outer radius  $d_0$ . Both relationships are linear, all input data are from Table 1 except radius  $d_0$ .

If radius  $d_0$  is equal to radius  $a_0$ , no constrained recovery occurs, and if radius  $d_0$  is equal to  $a_1$ , constrained recovery starts at temperature  $A_{\text{S}}$  and maximum possible stresses are generated. It is well known from literature (Borden, 1990; Proft and Duerig 1990) and experiments presented later in this work also confirm it, that relationships in Figure 6 are not linear in the whole range since from a specific radius  $d_0$  (or from specific contact strain) onwards the contact pressure  $p_0$  and temperature  $T_{\text{SE}}$  are more or less constant. In the commercial brochure of Intrinsic Devices Inc. the instruction is that their rings have to be heated up to  $165^\circ\text{C}$  for maximum

**Figure 3. Distribution of normal radial stress  $\sigma_r$  in both rings at temperatures  $T_{\text{SE}}$  and  $T_{\text{end}}$ .****Figure 4. Distribution of normal circular stress  $\sigma_{\varphi}$  in both rings at temperatures  $T_{\text{SE}}$  and  $T_{\text{end}}$ .****Figure 5. Distribution of effective stress  $\sigma_e$  in both rings at temperatures  $T_{\text{SE}}$  and  $T_{\text{end}}$ .**

stresses to be generated. This is roughly in agreement with the results in Figure 6.

The relationships between mass fraction of oriented martensite  $\xi$  and radius of the SMA ring at two different temperatures  $A_{\text{S}}$  and  $T_{\text{SE}}$  are presented in Figure 7. All input data are again from Table 1. As already noted, the structure of the SMA ring at temperature  $A_{\text{S}}$  is

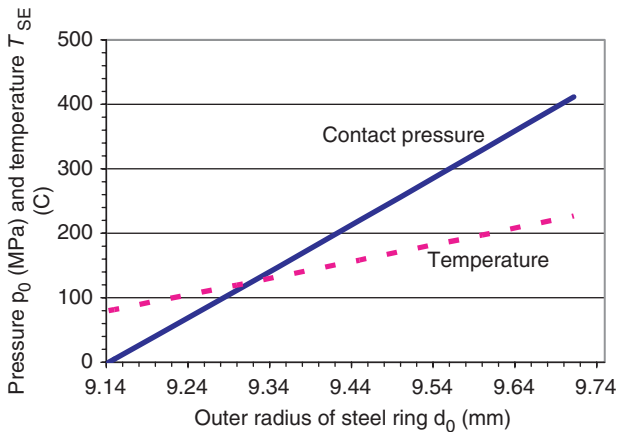


Figure 6. Contact pressure  $p_0$  at temperature  $T_{end}$  and temperature  $T_{SE}$  versus outer radius  $d_0$ .

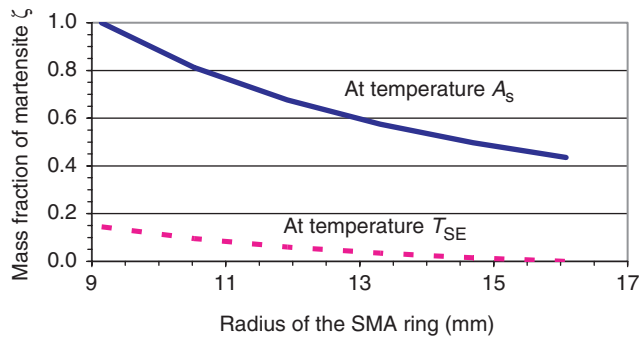


Figure 7. Mass fraction of oriented martensite  $\xi$  at the start of free recovery (temperature  $A_s$ ) and at the end of constrained recovery (temperature  $T_{SE}$ ) in the SMA ring.

assumed not to be 100%-oriented martensite since excessive stresses would be needed in the case of thick-walled SMA rings during the ‘widening’ process. Therefore only at inner radius  $a_0$  the structure is assumed to be 100%-oriented martensite. For simplicity reasons, the temperature  $T_{SE}$  at the end of constrained recovery process is calculated from the condition that at outer radius  $b_0$  the structure is 100%-austenite. The structure at all other radii is therefore a mixture of martensite and austenite as can be clearly seen in Figure 7.

It is essential for any mathematical model to be verified by experiments. Therefore, constrained recovery was measured in six commercial  $Ni_{48}Ti_{38}Nb_{14}$  SMA rings. One SMA ring was subjected to free recovery to obtain the data necessary for mathematical modeling. Six steel rings were used as mechanical obstacles. High quality steel was used (ISO: 36CrNiMo6,3,6) since only elastic deformations are considered in the model. The Young’s modulus and yield stress of three steel specimens were measured on ZWICK Z050 tensile test machine. The value of steel Young’s modulus is 195 GPa and yield stress is 970 MPa, which is well above the

Table 3. Material properties of SMA rings.

$M_S^0 = -80^\circ\text{C}$	$M_f^0 = -130^\circ\text{C}$	$A_S^0 = -70^\circ\text{C}$	$A_f^0 = 0^\circ\text{C}$
$A_S = 50^\circ\text{C}$	$A_f = 80^\circ\text{C}$	$E_A = 68 \text{ GPa}$	$\sigma_Y = 480 \text{ MPa}$
$\alpha_S = 1.1 \times 10^{-5} \text{ K}^{-1}$	$\nu_S = 0.3$	$M_d = 15^\circ\text{C}$	$C = 5.5 \text{ MPa/K}$

maximal effective stress in steel ring  $\sigma_e^{st}(c_0; T_{SE}) = 562.5 \text{ MPa}$  from Figure 5. This means that the assumption of elastic strains in the steel ring is reasonable. The Poisson’s ratio and linear thermal expansion coefficient of steel, which are used in the analytical model are taken from materials science handbook:  $\nu_{st} = 0.3$  and  $\alpha_{st} = 1.15 \times 10^{-5} \text{ K}^{-1}$ .

The material properties of SMA rings are presented in Table 3 and were provided by Intrinsic Devices Inc.

The austenite start and finish temperatures  $A_S^0$  and  $A_f^0$  are values of intact NiTiNb material. Using special pre-deformation treatment in the martensitic or stress-induced transformation temperature range (compared to the original  $A_S^0$ ) these temperatures are shifted to  $A_S$  and  $A_f$ , so that this material can be used at ambient temperatures (Melton et al., 1986). The pre-deformation relaxes the stored elastic strain energy in multi-variants martensites, and results in the increase of  $A_S$  and  $A_f$  (Piao et al., 1993). After the first temperature cycle,  $A_S$  and  $A_f$  are returned to original temperatures  $A_S^0$  and  $A_f^0$ . The value of the Young’s modulus of martensite  $E_M$  was not available, but it is well known (Borden, 1991) that it can be as low as 20 GPa. The Young’s modulus of austenite  $E_A$  was measured on intact (no special pre-deformation treatment)  $Ni_{48}Ti_{38}Nb_{14}$  wire specimens (diameter 4.54 mm) at temperature  $20^\circ\text{C}$  on ZWICK Z050 tensile test machine:  $E_A = 68 \text{ GPa}$ . In the mathematical model, the constant value of Young’s modulus was chosen to be  $E_S = 30 \text{ GPa}$ . This value is closer to  $E_M$ , since during constrained recovery the austenite part of the material is not contracting but actually extending. In this way the influence of  $E_A$  is relatively smaller than  $E_M$  and value  $E_S$  is chosen closer to the martensite value. One SMA ring ( $a_1 = 9.7015 \text{ mm}$  and  $b_1 = 16.515 \text{ mm}$ , martensite structure) was heated in teflon oil to temperature  $89^\circ\text{C}$  for 10 min and then cooled down to ambient temperature  $T_0 = 20^\circ\text{C}$ . No mechanical obstacle (steel ring) was used during this temperature cycle (free recovery). The inner and outer radii of SMA ring  $a_0$  and  $b_0$  were measured at  $T_0$  (austenite structure) by the DEA coordinate measuring machine:  $a_0 = 9.143 \text{ mm}$  and  $b_0 = 16.08 \text{ mm}$ . These values are used in the model as radii before the ‘widening’ process. Dimensions of six SMA rings and six steel rings, which were measured by the DEA coordinate measuring machine and used in the modeling process of constrained recovery are shown in Table 4.

The outer radius of the steel ring  $d_0$  in the table was chosen to contact the SMA ring at different contact

**Table 4. Dimensions of SMA and steel rings.**

	$a_1$ (mm)	$b_1$ (mm)	$c_0$ (mm)	$d_0$ (mm)
1	9.7015	16.514	8.285	9.2035
2	9.7165	16.5155	7.7205	9.252
3	9.711	16.516	7.2145	9.302
4	9.712	16.5145	7.2135	9.2995
5	9.707	16.515	6.9795	9.3525
6	9.708	16.5155	6.999	9.4035

**Table 5. Theoretical and experimental values of inner diameter  $2c$  and radial displacements at inner diameter  $2u^{st}$  of steel rings.**

	$T_C$ (°C)	$2c_{end}^{the}$ (mm)	$2c_{end}^{exp}$ (mm)	$2u_{the}^{st}$ (μm)	$2u_{exp}^{st}$ (μm)	Error (%)
1	76.73	16.538	16.532	-32	-38	-15.8
2	74.28	15.403	15.403	-38	-38	0
3	71.58	14.387	14.390	-42	-39	7.7
4	71.73	14.386	14.385	-41	-42	-2.4
5	68.84	13.910	13.919	-49	-40	22.5
6	66.15	13.937	13.954	-61	-44	38.6

temperatures  $T_C$ . The width of all SMA and steel rings was the same: 13.75 mm. Since biaxial stress state is assumed, the width has no influence on results.

The system SMA ring – steel ring was heated in teflon oil few degrees above calculated temperature  $T_{SE}$  for 10 min and then cooled down to the end temperature which was equal to the ambient temperature:  $T_{end} = T_0 = 20^\circ\text{C}$ . The inner diameters of the steel ring  $2c_{end}$  were measured then by the DEA coordinate measuring machine (error  $\pm 2 \mu\text{m}$ ) and were also calculated numerically (Table 5). The input data for numerical calculation were selected from Tables 1, 3, and 4.

The theoretical radial displacement  $u_{the}^{st}$  at inner radius  $c_0$  in Table 5 is calculated from the expression  $u_{the}^{st} = c_{end}^{the} - c_0$  and the measured one from the expression  $u_{exp}^{st} = c_{end}^{exp} - c_0$ . The error presented in the table is calculated using the expression  $err = 100 (u_{the}^{st} - u_{exp}^{st}) / u_{exp}^{st}$ . Figure 8 presents the relationship between the theoretical and experimental contact pressures at temperature  $T_{end}$  and the outer radii of steel rings  $d_0$ . The experimental contact pressures were not measured but were calculated from the measured radial displacements  $u_{exp}^{st}$  from Table 5. Some other calculated values are presented in Table 6. Contact pressures  $p_0(T_{SE})$  in this table were calculated from theory, while the last two columns are contact pressures at temperature  $T_{end}$  for theory and experiment, respectively.

From Figure 8 and Table 6 it can be clearly seen that the comparison between theory and experiment shows a good agreement for the first four examples when stresses

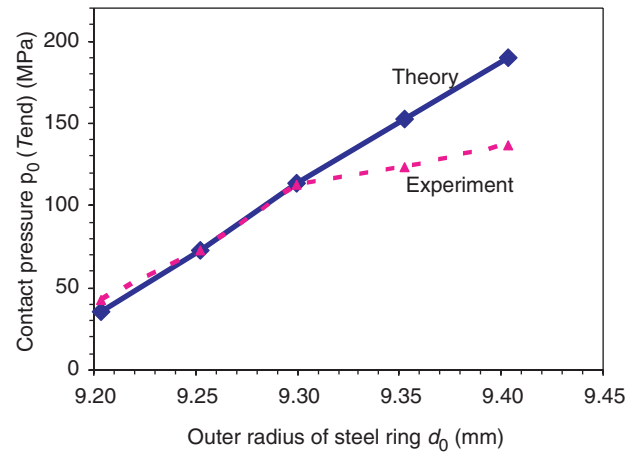


**Figure 8. Experimental and theoretical values of contact pressure versus outer radius  $d_0$  of steel rings.**

**Table 6. Calculated values of some characteristic properties of constrained recovery.**

	$T_{SE}$ (°C)	$\xi(a_0; T_{SE})$	$\sigma_e(T_{SE})$ (MPa)	$\sigma_e^{st}(T_{SE})$ (MPa)	$p_0(T_{SE})$ (MPa)	$p_0(T_{end})$ (MPa)	$p_0(T_{end})$ (MPa) exp
1	92.96	0.0477	79.16	380.83	36.11	35.76	42.37
2	105.76	0.0957	157.46	481.92	73.17	72.63	72.82
3	120.44	0.1468	246.67	572.05	113.97	113.22	104.95
4	119.70	0.1445	242.20	562.54	112.03	111.29	112.99
5	134.93	0.1969	334.63	694.77	153.92	152.96	123.72
6	148.15	0.2448	411.39	852.24	191.22	190.06	136.62

are lower. In the model, plastic strains are neglected in SMA rings, but at higher stresses this assumption is not good enough. For instance, instead of Equation (45) at higher stresses it should be written for circular strain in SMA rings that:

$$\varepsilon_\varphi = \frac{u}{r} = \lambda_M(1 + \alpha)\xi + \alpha_S(T - T_0) + \frac{1}{E_S}(\sigma_\varphi^{el} - \nu_S\sigma_r^{el}) + \varepsilon_\varphi^{pl} \tag{64}$$

where  $\varepsilon_\varphi^{pl}$  is the plastic circular strain. Effective stresses  $\sigma_e$  and  $\sigma_e^{st}$  in Table 6 are the maximal ones (at inner radii  $a_0$  and  $c_0$ , respectively). All six values of maximum effective stresses  $\sigma_e^{st}$  in steel are below the yield stress (970 MPa) and an assumption of elastic stress–strain state is justified. Even though effective stresses  $\sigma_e$  in SMA rings for the fifth and sixth examples are smaller than yield stress in Table 3, plastic strains may occur since yield stress defined in Table 3 is for austenite. The martensite yield stress for the tested SMA material should be smaller but was not available in literature.

**CONCLUSIONS**

A mathematical model for the analysis of the process of a biaxial constrained recovery in

thick-walled SMA ring was presented. The theory of generalized plasticity was used in modeling and as a mechanical obstacle causing constrained recovery in SMA ring, a steel ring was used. Final equations for stresses in a SMA ring are written in a closed form, but even though some simplifications were made, they cannot be written in a finite form. A mathematical model was verified by experiments and agreement is good for lower stresses when the SMA ring is in the elastic domain. When stresses are higher, unrecoverable processes occur in the SMA ring but these were neglected in the mathematical model. In future, it would be interesting to consider plastic strains in the SMA ring, Drucker–Prager effective stress

(Lubliner and Auricchio, 1996) instead of modified Tresca effective stress (9), exponential flow rule (Auricchio, 1995; Lubliner and Auricchio, 1996) instead of linear flow rule (11), and varying Young’s modulus during retransformation from martensite to austenite instead of a constant value  $E_S$  which was used in the present work.

**ACKNOWLEDGMENTS**

The authors gratefully acknowledge Mr. Tom Borden from Intrinsic Devices Inc. for providing SMA rings and the majority of the required data.

**APPENDIX**

In the expressions for radial and circular stresses in the SMA ring (49), (50), (59), and (60) seven integrals can be found, which can be solved, using the theorem of Chebyshev, in a closed and infinite form. Fortunately all these functions converge quite fast so that good results are obtained if first 15 terms in series ( $k=0, \dots, 14$ ) are applied. The integrals are:

$$\left\{ \begin{aligned} I_1(r) &= \int_{a_0}^r \rho^{\frac{1-\alpha}{1+\alpha}} \ln \frac{b_0^2 + \alpha \rho^2}{b_0^2 + \alpha a_0^2} d\rho \\ &= \frac{1+\alpha}{2} \left[ \left( r^{\frac{2}{1+\alpha}} - a_0^{\frac{2}{1+\alpha}} \right) \ln \frac{b_0^2}{b_0^2 + \alpha a_0^2} + \sum_{k=0}^{\infty} \frac{(-1)^k \alpha^{k+1} \left( r^{2k+\frac{4+2\alpha}{1+\alpha}} - a_0^{2k+\frac{4+2\alpha}{1+\alpha}} \right)}{(k+1)((1+\alpha)(k+1)+1)b_0^{2(k+1)}} \right] \end{aligned} \right. \tag{A1}$$

$$I_2(r) = \int_{a_0}^r \frac{\rho^{\frac{1-\alpha}{1+\alpha}}}{b_0^2 + \alpha \rho^2} d\rho = \frac{1+\alpha}{2} \sum_{k=0}^{\infty} \frac{(-\alpha)^k \left( r^{2k+\frac{2}{1+\alpha}} - a_0^{2k+\frac{2}{1+\alpha}} \right)}{((1+\alpha)k+1)b_0^{2(k+1)}} \tag{A2}$$

$$I_3(r) = \int_{a_0}^r \frac{\rho^{\frac{3+\alpha}{1+\alpha}}}{b_0^2 + \alpha \rho^2} d\rho = \frac{1+\alpha}{2} \sum_{k=0}^{\infty} \frac{(-\alpha)^k \left( r^{2k+\frac{4+2\alpha}{1+\alpha}} - a_0^{2k+\frac{4+2\alpha}{1+\alpha}} \right)}{((1+\alpha)(k+1)+1)b_0^{2(k+1)}} \tag{A3}$$

$$I_4(r) = \int_{a_0}^r \frac{\rho^{\frac{3+\alpha}{1+\alpha}}}{(b_0^2 + \alpha \rho^2)^2} d\rho = \frac{1+\alpha}{2} \sum_{k=0}^{\infty} \frac{(-\alpha)^k (k+1) \left( r^{2k+\frac{4+2\alpha}{1+\alpha}} - a_0^{2k+\frac{4+2\alpha}{1+\alpha}} \right)}{((1+\alpha)(k+1)+1)b_0^{2(k+2)}} \tag{A4}$$

$$\left\{ \begin{aligned} I_5(r) &= \int_{a_0}^r \rho^{-\frac{1+3\alpha}{1+\alpha}} \ln \frac{b_0^2 + \alpha \rho^2}{b_0^2 + \alpha a_0^2} d\rho \\ &= \frac{1+\alpha}{2} \left[ -\frac{1}{\alpha} \left( r^{-\frac{2\alpha}{1+\alpha}} - a_0^{-\frac{2\alpha}{1+\alpha}} \right) \ln \frac{b_0^2}{b_0^2 + \alpha a_0^2} + \sum_{k=0}^{\infty} \frac{(-1)^k \alpha^{k+1} \left( r^{2k+\frac{2}{1+\alpha}} - a_0^{2k+\frac{2}{1+\alpha}} \right)}{(k+1)((1+\alpha)k+1)b_0^{2(k+1)}} \right] \end{aligned} \right. \tag{A5}$$

$$I_6(r) = \int_{a_0}^r \frac{\rho^{-\frac{1+3\alpha}{1+\alpha}}}{b_0^2 + \alpha \rho^2} d\rho = \frac{1+\alpha}{2} \sum_{k=0}^{\infty} \frac{(-\alpha)^k \left( r^{2k-\frac{2\alpha}{1+\alpha}} - a_0^{2k-\frac{2\alpha}{1+\alpha}} \right)}{((1+\alpha)k-\alpha)b_0^{2(k+1)}} \tag{A6}$$

$$I_7(r) = \int_{a_0}^r \frac{\rho^{\frac{1-\alpha}{1+\alpha}}}{(b_0^2 + \alpha \rho^2)^2} d\rho = \frac{1+\alpha}{2} \sum_{k=0}^{\infty} \frac{(-\alpha)^k (k+1) \left( r^{2k+\frac{2}{1+\alpha}} - a_0^{2k+\frac{2}{1+\alpha}} \right)}{((1+\alpha)k+1)b_0^{2(k+2)}} \tag{A7}$$

## REFERENCES

- Auricchio, F. 1995. "Shape-memory Alloys: Applications, Micromechanics, Macromodelling and Numerical Simulations," Ph.D. Thesis, University of California at Berkeley.
- Auricchio, F. and Lubliner, J. 1997. "A Uniaxial Model for Shape-memory Alloys," *International Journal of Solids and Structures*, 34(27):3601–3618.
- Borden, T. 1990. "Shape Memory Alloy Fastener Rings," In: *Engineering Aspects of Shape Memory Alloys*, Butterworth-Heinemann.
- Borden, T. 1991. "Shape-Memory Alloys: Forming a Tight Fit," *Mechanical Engineering*, 113(10):67–72.
- Boyd, J.G. and Lagoudas, D.C. 1996a. "A Thermodynamical Constitutive Model for Shape Memory Materials. Part I. The Monolithic Shape Memory Alloy," *International Journal of Plasticity*, 12(6):805–842.
- Boyd, J.G. and Lagoudas, D.C. 1996b. "A Thermodynamical Constitutive Model for Shape Memory Materials. Part II. The SMA Composite Material," *International Journal of Plasticity*, 12(7):843–873.
- Brinson, L.C. 1993. "One-dimensional Constitutive Behavior of Shape Memory Alloys: Thermomechanical Derivation with Non-constant Material Functions and Redefined Martensite Internal Variable," *Journal of Intelligent Material Systems and Structures*, 4(2):229–242.
- Brocca, M., Brinson, L.C. and Bažant, Z.P. 2002. "Three-Dimensional Constitutive Model for Shape Memory Alloys Based on Microplane Model," *Journal of the Mechanics and Physics of Solids*, 50(5):1051–1077.
- Edwards, G.R., Perkins, J. and Johnson, J.M. 1975. "Characterizing the Shape Memory Effect Potential of Ni-Ti Alloys," *Scripta Metallurgica*, 9(11):1167–1171.
- Furuya, Y., Shimada, H., Tanahashi, Y., Matsumoto, M. and Honma, T. 1988. "Evaluation of Recovery Bending Force of Shape Memory Ni-Ti Alloy," *Scripta Metallurgica*, 22(6):751–755.
- Ghorashi, M. and Inman, D.J. 2004. "Shape Memory Alloy in Tension and Compression and its Application as Clamping Force Actuator in a Bolted Joint: Part 2 – Modeling," *Journal of Intelligent Material Systems and Structures*, 15(8):589–600.
- Hesse, T., Ghorashi, M. and Inman, D.J. 2004. "Shape Memory Alloy in Tension and Compression and its Application as Clamping Force Actuator in a Bolted Joint: Part 1 – Experimentation," *Journal of Intelligent Material Systems and Structures*, 15(8):577–587.
- Huang, M., Gao, X. and Brinson, L.C. 2000. "A Multivariant Micromechanical Model for SMAs Part 2. Polycrystal Model," *International Journal of Plasticity*, 16(10–11):1371–1390.
- Ivshin, Y. and Pence, T.J. 1994. "A Thermomechanical Model for a One Variant Shape Memory Material," *Journal of Intelligent Material Systems and Structures*, 5(4):455–473.
- Kafka, V. 1994. "Shape Memory: A New Concept of Explanation and of Mathematical Modelling: Part I: Micromechanical Explanation of the Causality in the SM Processes," *Journal of Intelligent Material Systems and Structures*, 11(5):809–814.
- Kapgan, M. and Melton, K.N. 1990. "Shape Memory Alloy Tube and Pipe Couplings," In: *Engineering Aspects of Shape Memory Alloys*, Butterworth-Heinemann.
- Kato, H., Inagaki, N. and Sasaki, K. 2004. "A One-Dimensional Modelling of Constrained Shape Memory Effect," *Acta Materialia*, 52(11):3375–3382.
- Kosel, F. and Videnic, T. 2007. "Generalized Plasticity and Uniaxial Constrained Recovery in Shape Memory Alloys," *Mechanics of Advanced Materials and Structures*, 14(1):3–12.
- Lagoudas, D.C., Entchev, P.B., Popov, P., Patoor, E., Brinson, L.C. and Gao, X. 2006. "Shape Memory Alloys, Part II: Modeling of Polycrystals," *Mechanics of Materials*, 38(5–6):430–462.
- Leclercq, S. and LExcellent, C. 1996. "A General Macroscopic Description of the Thermomechanical Behavior of Shape Memory Alloys," *Journal of the Mechanics and Physics of Solids*, 44(6):953–980.
- Liang, C. and Rogers, C.A. 1990. "One-dimensional Thermomechanical Constitutive Relations for Shape Memory Materials," *Journal of Intelligent Material Systems and Structures*, 1(2):207–234.
- Lubliner, J. and Auricchio, F. 1996. "Generalized Plasticity and Shape-memory Alloys," *International Journal of Solids and Structures*, 33(7):991–1003.
- Madangopal, K., Ganesh Krishnan, R. and Banerjee, S. 1988. "Reversion Stresses in Ni-Ti Shape Memory Alloys," *Scripta Metallurgica*, 22(10):1593–1598.
- Melton, K.N., Simpson, J. and Duerig, T.W. 1986. "A New Wide Hysteresis NiTi Based Shape Memory Alloy and its Applications," In: *Proceedings of the International Conference on Martensitic Transformations (ICOMAT-86)*, The Japan Institute of Metals, 1053–1058.
- Mohamed, H.A. 1978. "Determination of the Recovery Stresses Developed by Shape Memory Alloys," *Journal of Materials Science*, 13(12):2728–2730.
- Nagaya, K. and Hirata, Y. 1992. "Analysis of a Coupling Made of Shape Memory Alloy and its Dynamic Response Due to Impacts," *Journal of Vibration and Acoustics*, 114(3):297–304.
- Novak, V. and Šittner, P. 2004. "Micromechanics Modelling of NiTi Polycrystalline Aggregates Transforming Under Tension and Compression Stress," *Materials Science and Engineering A*, 378(1–2):490–498.
- Otsuka, K. and Wayman, C.M. 1997. *Shape Memory Materials*, Cambridge University Press.
- Panoskaltis, V.P., Bahuguna, S. and Soldatos, D. 2004. "On the Thermomechanical Modeling of Shape Memory Alloys," *International Journal of Non-linear Mechanics*, 39(5):709–722.
- Patoor, E., Lagoudas, D.C., Entchev, P.B., Brinson, L.C. and Gao, X. 2006. "Shape Memory Alloys, Part I: General Properties and Modeling of Single Crystals," *Mechanics of Materials*, 38(5–6):391–429.
- Piao, M., Otsuka, K., Miyazaki, S. and Horikawa, H. 1993. "Mechanism of the  $A_s$  Temperature Increase by Pre-deformation in Thermoelastic Alloys," *Materials Transactions JIM*, 34(10):919–929.
- Proft, J.L. and Duerig, T.W. 1990. "The Mechanical Aspects of Constrained Recovery," In: *Engineering Aspects of Shape Memory Alloys*, Butterworth-Heinemann.
- Stalmans, R., Delaey, L. and Van Humbeeck, J. 1997. "Generation of Recovery Stresses: Thermodynamic Modelling and Experimental Verification," *Journal de Physique IV*, 7(C5):47–52.
- Stalmans, R., Van Humbeeck, J. and Delaey, L. 1995. "Thermodynamic Modelling of Shape Memory Behaviour: Some Examples," *Journal de Physique IV*, 5(C8):203–208.
- Šittner, P., Vokoun, D., Dayananda, G.N. and Stalmans, R. 2000. "Recovery Stress Generation in Shape Memory  $Ti_{50}Ni_{45}Cu_5$  Thin Wires," *Materials Science and Engineering A*, 286(2):298–311.
- Tanaka, K. 1986. "A Thermomechanical Sketch of Shape Memory Effect: One-dimensional Tensile Behavior," *Research Mechanics*, 18(3):251–263.
- Thamburaja, P. and Anand, L. 2001. "Polycrystalline Shape-Memory Materials: Effect of Crystallographic Texture," *Journal of the Mechanics and Physics of Solids*, 49(4):709–737.
- Tokuda, M., Ye, M., Takakura, M. and Šittner, P. 1998. "Calculation of Mechanical Behaviors of Shape Memory Alloy Under Multi-axial Loading Conditions," *International Journal of Mechanical Sciences*, 40(2–3):227–235.
- Tsoi, K.A., Stalmans, R. and Schrooten, J. 2002. "Transformational Behaviour of Constrained Shape Memory Alloys," *Acta Materialia*, 50(14):3535–3544.
- Videnic, T. 2004. "Constrained Recovery in Shape Memory Alloys," Ph.D. Thesis, University of Ljubljana (in Slovene).
- Zhu, J.J. and Liew, K.M. 2004. "Describing the Morphology of 2H Martensite Using Group Theory Part I: Theory," *Mechanics of Advanced Materials and Structures*, 11(3):197–225.